

Layer VQE: A Variational Approach for Combinatorial Optimization on Noisy Quantum Computers

Xiaoyuan Liu,¹ Anthony Angone,² Ruslan Shaydulin,³ Ilya Safro,¹ Yuri Alexeev,⁴ and Lukasz Cincio⁵

¹*University of Delaware, Newark, DE 19716, USA*

²*School of Computing, Clemson University, Clemson, SC 29634, USA*

³*Mathematics and Computer Science Division,*

Argonne National Laboratory, Lemont, IL 60439, USA

⁴*Computational Science Division, Argonne National Laboratory, Lemont, IL 60439, USA*

⁵*Theoretical Division, Los Alamos National Laboratory, Los Alamos, NM 87545, USA*

Combinatorial optimization on near-term quantum devices is a promising path to demonstrating quantum advantage. However, the capabilities of these devices are constrained by high noise levels and limited error mitigation. In this paper, we propose an iterative Layer VQE (L-VQE) approach, inspired by the Variational Quantum Eigensolver (VQE). We present a large-scale numerical study, simulating circuits with up to 40 qubits and 352 parameters, that demonstrates the potential of the proposed approach. We evaluate quantum optimization heuristics on the problem of detecting multiple communities in networks, for which we introduce a novel qubit-frugal formulation. We numerically compare L-VQE with QAOA and demonstrate that QAOA achieves lower approximation ratios while requiring significantly deeper circuits. We show that L-VQE is more robust to sampling noise and has a higher chance of finding the solution as compared with standard VQE approaches. Our simulation results show that L-VQE performs well under realistic hardware noise.

I. INTRODUCTION

Recent advances in quantum computing hardware open the possibility of demonstrating quantum advantage in practical applications [1, 2]. A promising target application domain is combinatorial optimization, with problems becoming classically intractable (in the current state of theory) to solve exactly even for moderately sized instances. This situation suggests that the requirement for the number of qubits needed to tackle certain classically hard combinatorial optimization problems is relatively low, leading to the possibility of noisy intermediate-scale quantum (NISQ) [3] devices becoming competitive with classical state-of-the-art methods for such problems.

Near-term quantum devices are expected to have high noise levels, and only partial error mitigation is currently possible. This situation leads to a constraint on the maximum depth of the quantum circuit that can be reliably executed on NISQ devices. This constraint motivated the development of a number of hybrid quantum-classical algorithms for optimization, most notably the Quantum Approximate Optimization Algorithm (QAOA) [4, 5] and variational quantum algorithms for optimization [6–8]. These algorithms execute only a short parameterized circuit on the quantum computer and use a classical outer-loop procedure to find “good” parameters [9]. The short parameterized circuit is often referred to as the ansatz. The goal of the outer-loop procedure, in general, is to find parameters such that the output of the quantum circuit includes high-quality solutions to the combinatorial optimization problem being solved.

The choice of the ansatz is a key problem in hybrid algorithms. Two main concerns are the *expressivity* and the *trainability* of the chosen ansatz. First, the ansatz has to be sufficiently expressive, meaning that there should exist parameters with which the ansatz prepares a state suitably close to the solution of the problem. Second, the ansatz has to be trainable, meaning that sufficiently good parameters have to be feasible to find [10].

For combinatorial optimization problems, the solution is classical; in other words, it is a computational basis state. Therefore the first criterion, the expressivity of the ansatz, reduces to the ability to prepare a state with sufficiently large overlap with the computational basis state encoding the solution of the problem. This means that the ansatz can be sufficiently expressive without generating any entanglement or having any quantum properties whatsoever: one layer of single-qubit rotations is sufficient to prepare an arbitrary computational basis state. Such ansätze may not be trainable, however. Their structure enforces localized optimization, which is prone to local minima. As we discuss below, that class of ansätze may be extended to enhance trainability by introducing a correlation between distant parts of the system. A commonly used

class of highly expressive ansätze are those with alternating layers of single-qubit and two-qubit gates, where the two-qubit gates are aligned with the connectivity available on the hardware. These ansätze are known as quantum neural networks [11] or hardware-efficient ansätze [12]. An alternative and “natural” approach is the Hamiltonian-evolution ansatz used in QAOA. Such ansätze can be less expressive, however, since the state it has to prepare is a nontrivial entangled state due to the symmetry-preserving properties of the ansatz [13]. This observation has been used by Bravyi et al. [14] to show that because of the \mathbb{Z}_2 symmetry of the ansatz, QAOA with constant depth is outperformed by the classical Goemans–Williamson algorithm for MaxCut. As a result, QAOA needs a comparatively large circuit depth to achieve the same (classical) expressivity as compared with hardware-efficient ansatz.

For ansätze with a large number of parameters, the high-quality parameters are typically found by using a classical optimizer. Thus the second criterion, the trainability of the ansatz, is typically framed in terms of the cost function landscape that the classical outer-loop routine has to optimize over. Recent results show that highly expressive ansätze such as hardware-efficient ansätze suffer from “barren plateaus” in the optimization landscape, making finding high-quality parameters intractable [11, 15–24]. At the same time, a series of recent results show that because of the structured nature of the ansatz used in QAOA, one may be able to find high-quality parameters by using machine learning approaches [25–27] or by restricting the parameters to a specific physically motivated class [28–30]. Note that our notion of trainability is different from the one commonly used when discussing effects such as “barren plateaus.” In fact, it is more general: under our definition, a circuit may have large gradients for the whole parameter space and still not be trainable.

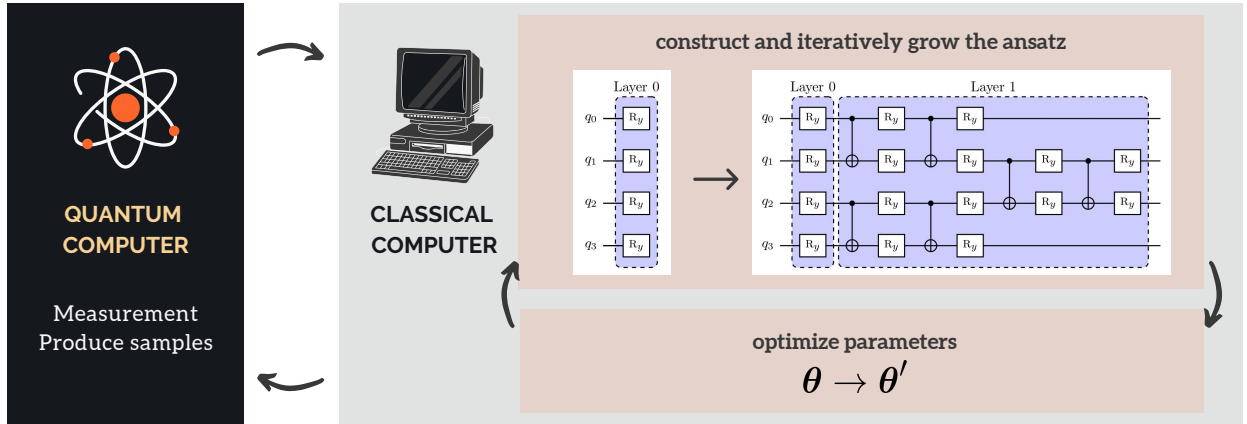


FIG. 1: Layer-VQE: start from a simple and shallow ansatz with one R_y act on each qubit; optimize and update the parameters; after some predefined number of iterations; increment the size of the ansatz; optimize and update all parameters. The ansatz can be incremented multiple times.

In this paper, we propose a practical approach to combinatorial optimization on near-term quantum computers. We introduce an iterative approach, which we call Layer VQE (L-VQE), inspired by recent advances in hybrid quantum-classical algorithms with an adaptive ansatz [7, 31, 32]. In L-VQE, we start with one layer of parameterized rotations and increment the size of the ansatz systematically by introducing entangling gates and additional parameterized rotations. To heuristically decrease the likelihood of getting trapped in a local optimum of the parameters, we increment the ansatz before reaching convergence. To guarantee that at each step the quality of the solution does not decrease, we initialize the added ansatz such that it evaluates to identity. We work with qubits aligned in a chain and assume nearest neighbor connectivity. This allows us to consider large problems by using tensor network techniques to simulate circuits. We expect that in practical applications on real quantum hardware, one would organize ansatz layers according to (typically two-dimensional) qubit connectivity to further enhance circuit expressiveness. Quantum circuits on such layouts cannot be in general classically efficiently simulated and are thus not considered in the present study.

Fig. 1 gives a schematic presentation of L-VQE. We study the algorithm for the problem of detecting k

communities in networks, and we propose a novel qubit-frugal formulation with many-body interactions in the Hamiltonian. For a network with n nodes, $n \lceil \log_2 k \rceil$ qubits are required for the circuit. We present a large-scale numerical study of the proposed approach, simulating circuits with up to 40 qubits and 352 rotational gates (i.e., parameters). Our numerical simulation results show that the proposed approach achieves a higher approximation ratio compared with QAOA while requiring significantly lower circuit depth. The proposed approach is more robust to sampling noise and performs better than hybrid approaches with a fixed ansatz. Moreover, we show that the proposed approach performs well under realistic hardware noise.

The rest of the paper is organized as follows. In Section II we review the relevant background of solving combinatorial optimizations on quantum computers. In Section III we review related work. Section IV introduces our L-VQE approach, and in Section V we discuss our novel formulation of the k -community detection problem. Section VI presents our numerical simulation results and in Section VII we summarize our conclusions.

II. BACKGROUND

We begin by briefly reviewing our notion of combinatorial optimization on quantum computers and relevant concepts. Suppose we have an objective function $C(x)$ defined on the Boolean cube $x = \{x_i\}_{i=1}^n \in \{0, 1\}^n$ and a corresponding optimization problem

$$\max_{x \in \{0, 1\}^n} C(x), \quad (1)$$

where the objective function $C(x)$ can be formulated in the following form:

$$C(x) = \sum_q w_q \prod_{i \in q} x_i \prod_{j \notin q} (1 - x_j). \quad (2)$$

Here, $q \subset \{1, 2, \dots, n\}$ are given index sets, and w_q are given coefficients. The objective function $C(x)$ is said to be *faithfully represented* by a Hamiltonian \mathcal{H} if it acts as $\mathcal{H}|x\rangle = C(x)|x\rangle$ for each $x \in \{0, 1\}^n$. For a function given in the form (2), such a Hamiltonian representation can be constructed by substituting every x_i with the matrix $x_i \rightarrow \frac{1}{2}(\mathbb{I} - Z_i)$, where \mathbb{I} is the identity matrix and Z_i is the Pauli Z operator that acts on qubit i :

$$\mathcal{H} = \sum_q w_q \prod_{i \in q} \frac{\mathbb{I} - Z_i}{2} \prod_{j \notin q} \frac{\mathbb{I} - Z_j}{2}. \quad (3)$$

Note that the operator $\mathcal{H} \in \mathbb{C}^{2^n}$ is never constructed explicitly. Instead, we construct a compact representation of it as a combination of Pauli Z operators.

A. Combinatorial Optimization on Near-Term Quantum Computers

The two most prominent candidate algorithms for combinatorial optimization on noisy near-term quantum computers are the Variational Quantum Eigensolver (VQE, originally proposed in the context of quantum chemistry [33]) and the Quantum Approximate Optimization Algorithm (QAOA) [4]. Both algorithms are hybrid quantum-classical algorithms that combine a parameterized trial $|\psi(\theta)\rangle$ state prepared on a quantum computer with a classical routine used to find high-quality parameters θ . The goal is to find parameters θ such that when the state $|\psi(\theta)\rangle$ is measured, the measurement result corresponds to a good solution of the classical optimization problem. The parameterized trial state $|\psi(\theta)\rangle$ is commonly called the ansatz.

In VQE, for optimization the ansatz is frequently tailored to the hardware [8, 34], and the parameters θ are found by using a classical outer-loop optimizer. The expectation value $\langle \psi(\theta) | \mathcal{H} | \psi(\theta) \rangle$ is commonly

used as the metric for the optimizer, although other approaches have been suggested [35]. QAOA uses a problem-dependent ansatz given by

$$|\psi_p(\boldsymbol{\gamma}, \boldsymbol{\beta})\rangle = e^{-i\beta_p B} e^{-i\gamma_p \mathcal{H}} \dots e^{-i\beta_1 B} e^{-i\gamma_1 \mathcal{H}} |+\rangle^{\otimes n}, \quad (4)$$

where $B = \sum_{i=1}^n x_i$ is the mixing Hamiltonian, x_i is the Pauli x operator acting on qubit i , \mathcal{H} is the Hamiltonian faithfully representing the objective function, and p is a parameter controlling the depth. The special structure of the QAOA ansatz enables finding high-quality parameters $\boldsymbol{\gamma}, \boldsymbol{\beta}$ purely classically in many settings [4, 36, 37] or using very few iterations of the outer-loop optimizer [25, 38, 39].

We evaluate the quality of the final quantum state $|\psi(\boldsymbol{\theta})\rangle$ by computing the approximation ratio ρ defined as follows:

$$\rho = \frac{\langle \psi(\boldsymbol{\theta}) | \mathcal{H} | \psi(\boldsymbol{\theta}) \rangle}{C_{\text{bkv}}}, \quad (5)$$

where C_{bkv} is the global optimum of the objective function $C(x)$ or the best known value, since when the size of the problem gets larger, the global optimal $\max_{x \in \{0,1\}^n} C(x)$ may not be accessible.

B. The k -Community Detection

The k -community detection, also known as modularity clustering, is a famous problem in network science. The goal is to partition a network into k communities such that the modularity metric [40] is maximized. Intuitively, when modularity with respect to a partition of the network is large, the connectivity between nodes inside each community is dense while the connectivity between each community is sparse. Modularity, when maximized, leads to the appearance of communities in a given network. It is defined as the fraction of the edges that fall within the given groups minus the expected fraction if edges were distributed at random.

For a formal definition, let $G = (V, E)$ be an undirected simple graph with $|V| = n$ nodes and $|E| = m$ edges. The adjacency matrix of G is denoted by $A = \{A_{u,v}\}_{1 \leq u,v \leq n}$, where $A_{u,v} = 1$ if there is an edge between node u and node v , and 0 otherwise. The degree of a node v is denoted by d_v . A k -community clustering $\mathcal{C} = \{C_1, \dots, C_k\}$ is a partition of V into k disjoint sets, namely, $\bigcup_{i=1}^k C_i = V$, and $C_i \cap C_j = \emptyset$ for all $1 \leq i \neq j \leq k$. Furthermore, c_v denotes the membership of node v for a given clustering; that is, if $v \in C_i$, then $c_v = i$. The modularity of a clustering \mathcal{C} is given by:

$$\mathcal{Q}(\mathcal{C}) = \frac{1}{2m} \sum_{u,v=1}^n B_{u,v} \delta(c_u, c_v), \quad (6)$$

where the modularity matrix B is given by $B_{u,v} = A_{u,v} - \frac{d_u d_v}{2m}$, $1 \leq u, v \leq n$, and δ is the Kronecker delta:

$$\delta(c_u, c_v) = \begin{cases} 1, & \text{if } c_u = c_v \\ 0, & \text{otherwise.} \end{cases} \quad (7)$$

Our goal is to find the clustering \mathcal{C} such that the modularity is maximized:

$$\text{argmax}_{\mathcal{C}} \mathcal{Q}(\mathcal{C}).$$

The problem has applications in chemistry [41], biology [42], social sciences [43], and other fields. Solving the modularity maximization problem to optimality is NP-complete [44].

III. RELATED WORK

A. Hybrid Quantum-Classical Algorithms

The question of ansatz choice is central to the success of hybrid quantum-classical methods introduced in Section II A. In VQE, the choice of the ansatz determines the expressivity and trainability of the trial

state; therefore, the quality of VQE is only as good as the ansatz. Different strategies of parameterizing the ansatz and updating the parameters will also affect the performance of the algorithm. While being able to reach any state requires a circuit with exponential depth, shallow circuits are preferred in applications, especially if the goal is to run the circuits on the modern NISQ devices. McClean et al. [11] show that with random parameterized circuit initialization, the exponential dimension of the Hilbert space and the gradient estimation complexity make the optimization impossible for deep circuits. Moreover, Wang et al. [45] show that another type of “barren plateau” is induced by hardware noise. More specifically, given local Pauli noise, the gradient vanishes exponentially with the depth of the circuits. Similar results have been demonstrated for QAOA [46].

Recently, a number of approaches have been proposed that attempt to overcome these limitations by using an adaptive or iteratively constructed ansatz. In conventional VQE approaches, the wave function ansatz (such as the unitary coupled cluster (UCC) ansatz [33] or hardware-efficient ansatz [12]) is preselected and fixed upfront. To address the limitation of the preselected ansatz, Grimsley et al. propose an adaptive variational algorithm ADAPT-VQE [31] that generates an ansatz with a small number of parameters and grows it systematically. This approach performs better than a UCC ansatz approach in terms of both circuit depth and accuracy.

With the same spirit, Zhu et al. propose an adaptive version of QAOA, called ADAPT-QAOA [7]. Compared with the standard QAOA ansatz, which alternates between the predefined exponentiated cost and mixing Hamiltonian operator, ADAPT-QAOA grows the ansatz with two operators at a time. It also uses a gradient criterion to select the mixing operator from a predefined operator pool. On a class of MaxCut graph problems, ADAPT-QAOA demonstrates faster convergence while also reducing the number of optimization parameters and the CNOT gate counts, compared with standard QAOA. Skolik et al. [32] propose a layer-wise learning strategy that grows the circuit depth incrementally during optimization and only updates subsets of parameters in training. However, a recent paper [22] shows that this type of layer-wise training strategy, namely, training a circuit piecewise in sequence, could encounter abrupt transitions in the training process as the depth of the circuit grows.

B. Community Detection

Community detection has been extensively studied classically [40, 47], as well as by using the D-wave quantum annealer [48–51] and QAOA [49, 51, 52]. In these hybrid quantum-classical approaches, the optimization problem is encoded as an Ising model Hamiltonian that has only two-body terms. In the formulations, for a graph with n vertices, solving the 2-community modularity maximization problem requires n qubits, where each qubit encodes the membership of a node. For the k -community problem, to encode the membership of each node, one will need to associate k qubits to each node, while introducing quadratic penalty constraints into the Ising Hamiltonian to enforce that each node belongs to only one community. The formulation requires kn qubits.

IV. LAYER VQE

We advocate an iterative hybrid approach to quantum optimization on NISQ devices, which we call Layer VQE. L-VQE combines ideas from recent developments in adaptive variational algorithms, such as [7, 31, 32]. In this section, we describe L-VQE in detail.

Suppose we use a problem encoding that requires n qubits. We start the algorithm with an ansatz with no entangling gates and one R_y gate acting on each qubit, where R_y is the single qubit rotation through an angle θ around the y -axis, the unitary matrix is defined as $R_y(\theta) \equiv e^{-i\frac{\theta}{2}\Upsilon}$, and Υ is the Pauli Υ operator. The parameters of these R_y gates are initialized uniformly randomly on $[0, 2\pi]$. We denote the parameters for this layer of gates (*Layer* θ in Fig. 2) as θ_0 and the layer as $U_0(\theta_0)$. The quantum state after applying the circuit to the initial state $|0\rangle$ is denoted as $|\psi_0(\theta_0)\rangle \equiv U_0(\theta_0)|0\rangle$. We then proceed to the conventional VQE routine and iteratively update the parameters θ_0 to minimize the cost function $\langle\psi_0(\theta_0)|\mathcal{H}|\psi_0(\theta_0)\rangle$. In conventional VQE, this iterative procedure is run until convergence; but in L-VQE, we stop after a fixed

number of iterations and then add another set of gates to the ansatz. The conventional strategy can indeed produce a better result at this step, but after adding the new set of gates, it may more easily get trapped in a local minimum in the subsequent optimization procedure. In our experiments, the number of iterations is picked empirically and increases linearly as system size grows.

The newly added set of gates includes the R_y gates and CNOT gates that act on nearest-neighbor qubits. Another way to describe this whole procedure is that we embed the obtained parameterized circuit into a deeper circuit. We denote this newly added layer of the circuit $U_1(\theta_1)$, (*Layer 1* in Fig. 2). The newly added parameters θ_1 are initialized as zero. Note that here since $R_y(0) = I$ and $\text{CNOT}^2 = I$, where I is the identity matrix, the quantum state becomes

$$|\psi_1(\theta_0, \theta_1)\rangle \equiv U_1(\theta_1)U_0(\theta_0)|0\rangle = U_0(\theta_0)|0\rangle = |\psi_0(\theta_0)\rangle. \quad (8)$$

Therefore, initializing the newly added parameters as zeros guarantee that the cost function that we are optimizing will not change after adding this new layer. However, one may add small random perturbation to the parameters before optimization is continued. In that sense, θ_1 are not initialized with zero but with small random numbers. As we proceed to the optimization process, iteratively updating the parameters θ_0, θ_1 to minimize the cost function $\langle\psi_1(\theta_0, \theta_1)|\mathcal{H}|\psi_1(\theta_0, \theta_1)\rangle$, initializing with small random numbers may be useful to avoid local minima and speed up the optimization in general. At this point, we can either let the optimization run until convergence or repeat the previous process, stop at a fixed number of iterations, and add another set of gates to the circuit and then optimize. The pseudo code of the algorithm is presented in Algorithm 1.

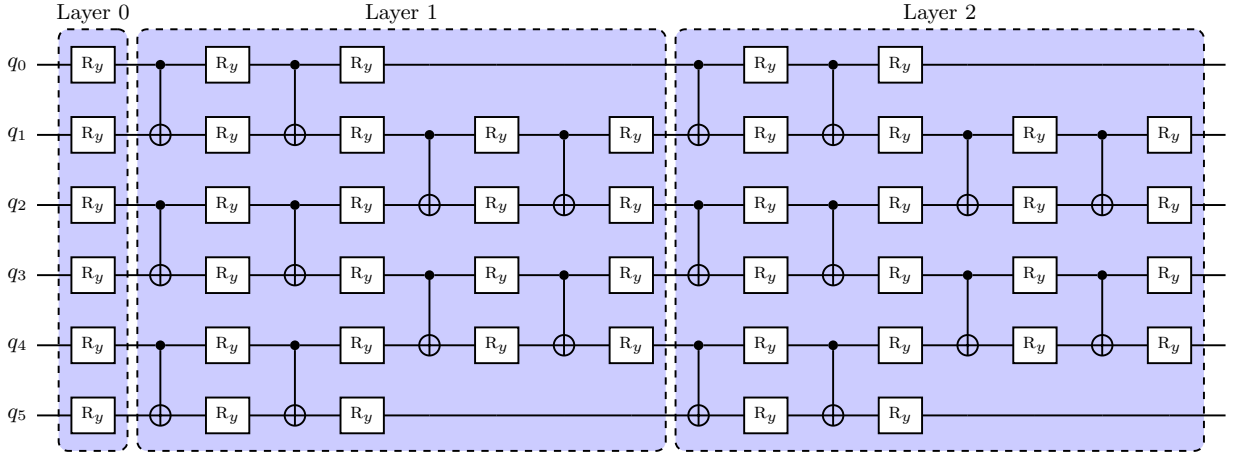


FIG. 2: L-VQE ansatz for a 6-qubit quantum state. R_y denotes rotation around the y -axis defined as $R_y(\theta) \equiv e^{-i\frac{\theta}{2}\sigma_y}$. Every R_y contains a parameter that is optimized over in the outer loop.

Algorithm 1 L-VQE with ℓ layers

- 1: Initialize the ansatz with one R_y acting on each qubit.
 - 2: Update the parameters to minimize $\langle\psi_0(\theta)|\mathcal{H}|\psi_0(\theta)\rangle$; stop after k_0 iterations (before reaching convergence).
 - 3: **for** $l = 1, \dots, \ell$ **do**
 - 4: Add a new layer to the ansatz, and initialize them such that they evaluate to identity.
 - 5: Update all parameters to minimize $\langle\psi_l(\theta)|\mathcal{H}|\psi_l(\theta)\rangle$; stop after k_l iterations (before reaching convergence).
 - 6: **end for**
 - 7: Update all parameters to minimize $\langle\psi(\theta)|\mathcal{H}|\psi(\theta)\rangle$ until convergence.
-

In simulations, the cost function $\langle\psi(\theta)|\mathcal{H}|\psi(\theta)\rangle$ can be evaluated exactly, but in practical applications we will repeat the state preparation and measurement multiple times to generate a number of samples, and we

use the samples to estimate the cost function. In our experiments we investigate the performance of the algorithm in both cases.

Similar to ADAPT-VQE [31] and ADAPT-QAOA [7], we grow the size of the ansatz as we iteratively update the parameters. The added parameterized ansatz is initialized such that the new circuit parts evaluate to identity in order to avoid deterioration of the optimization. In ADAPT-VQE and ADAPT-QAOA, however, the algorithm will identify an operator that has the largest gradient from a collection of operators and then add this operator to the ansatz. In L-VQE, we define the newly added ansatz upfront. Unlike layer-wise learning [32] where only subsets of the parameters are updated in training, we optimize over all parameters and thereby may reduce the limitations of the lack of layer-wise trainability [22]. In addition, unlike previous approaches, we grow the size of the ansatz before the convergence is reached, which again may be beneficial to avoid local minima.

V. THE k -COMMUNITY DETECTION

We propose a novel qubit-frugal formulation for the k -community detection problem. When the problem is to divide the network into two communities, namely, with $k = 2$, we can associate a binary variable with each node $v \in V$ such that

$$x_v = \begin{cases} 1, & \text{if } c_v = 1 \\ 0, & \text{if } c_v = 2. \end{cases}$$

Then, we can rewrite the Kronecker delta (7) in terms of these binary variables:

$$\delta(c_u, c_v) = \delta(x_u, x_v) = 2x_u x_v - x_u - x_v + 1. \quad (9)$$

Plugging (9) into (6) leads to the expression of modularity:

$$\mathcal{Q}(\mathcal{C}) = \frac{1}{2m} \sum_{u,v=1}^n B_{u,v} (2x_u x_v - x_u - x_v + 1).$$

For larger k , we can use a binary encoding by associating $N = \lceil \log_2 k \rceil$ binary variables $\{x_{j,v}\}_{j=1}^N \subset \{0,1\}^N$ with each node $v \in V$. We can rewrite the membership of node v as

$$c_v = \sum_{j=1}^N 2^{j-1} x_{j,v}.$$

Again, we can rewrite the Kronecker delta (7) in terms of these binary variables:

$$\delta(c_u, c_v) = \prod_{j=1}^N \delta(x_{j,u}, x_{j,v}) = \prod_{j=1}^N (2x_{j,u} x_{j,v} - x_{j,u} - x_{j,v} + 1). \quad (10)$$

Plugging (10) into (6), we obtain for the modularity

$$\mathcal{Q}(\mathcal{C}) = \frac{1}{2m} \sum_{u,v=1}^n B_{u,v} \prod_{j=1}^N (2x_{j,u} x_{j,v} - x_{j,u} - x_{j,v} + 1). \quad (11)$$

Following the construction described in Section II, maximizing the modularity in (11) can be formulated in terms of finding the ground state of the following Hamiltonian,

$$\mathcal{H} = -\frac{1}{2m} \sum_{u,v=1}^n B_{u,v} \prod_{j=1}^N \frac{I + Z_{j,u} Z_{j,v}}{2}, \quad (12)$$

where binary variables $x_{j,v}$ have been substituted with $\frac{1}{2}(I - Z_{j,v})$, $\forall j \in \{1, 2, \dots, N\}$, $\forall v \in V$. Here, $Z_{j,v}$ is the Pauli Z operator that acts on qubit (j, v) .

Other formulations have been proposed to tackle the problem for specific quantum architectures. Ushijima-Mwesigwa et al. [50] use an Ising Hamiltonian formulation to detect two communities using quantum annealing on the D-Wave system, which requires n qubits. Negre et al. [48] extend it to detect k communities, which requires kn qubits. In contrast, the Hamiltonian we propose in this work requires only $n \lceil \log_2 k \rceil$ qubits thanks to the encoding introduced above. A possible downside of our formulation is that we now have many-body interactions in the Hamiltonian, which make it harder to implement compared with the 2-body terms in existing works.

VI. EXPERIMENTS

In this section we present the numerical results. Since QAOA is considered the leading approach for combinatorial optimization on NISQ devices, we begin in Section VIA with a numerical comparison of L-VQE and QAOA. We then compare L-VQE with the second leading approach, which is VQE in Section VIB. To highlight the potential of the proposed L-VQE approach on NISQ devices, we present some further evidence in Section VIC. This includes a scalability analysis and simulation results of L-VQE on a trapped ion noisy quantum simulator with a realistic noise level. To highlight the importance of entanglement for optimization, in Section VID we present results comparing VQE with and without entanglement.

A. L-VQE and QAOA

For the first set of experiments, we run simulations for the L-VQE and QAOA algorithm with the proposed Hamiltonian (12). The goal is to find a clustering of up to 4 communities that maximize the modularity. We are thus simulating $2n$ qubits for a graph with n vertices. For L-VQE, we run our simulations of the quantum circuits in MATLAB. We use matrix product states techniques to simulate quantum circuits, which allows to reach large system sizes (up to 40 qubits and 352 parameters). We also represent the Hamiltonian in the form of a matrix product operator [53, 54]. For the classical optimization, we use a sequential minimal optimizer (SMO) [55]. For QAOA, we use the high-performance simulator Qiskit Aer [56] to simulate QAOA circuits. Because of the simulation complexity and the need to optimize parameters for the benchmark instances, we limit the simulation to 20 qubits. For optimization in QAOA, we use COBYLA [57, 58] implemented in the SciPy [59] package and also use COBYLA as a local optimizer in the libEnsemble [60] implementation of APOSMM [61, 62]. Given a fixed number of iterations, APOSMM as a multistart method will run the local optimizer until convergence and then restart the optimization. This approach has been shown to work well in our previous work [39].

We first generate a random graph with 7 vertices, shown in the inset of Fig. 3 (a), simulating 14 qubits. The maximal modularity with up to 4 communities of this graph can be found by brute force (0.1790). We report the approximation ratio ρ (defined in (5)) found by QAOA in Fig. 3 (a). We first run QAOA with p ranging from 1 to 30 for 10 times for each p , and we use COBYLA to optimize. Each run is given a different random seed and run until convergence. In Fig. 3 (a) we report the best approximation ratio we find from the 10 runs. Note that local optimizers such as COBYLA cannot guarantee to find the optimal parameters, especially as p increases. This is the reason that the data points of approximation ratio do not grow monotonically with p . Therefore, to further improve the optimizer, we use the multistart method APOSMM with COBYLA, which uses an ensemble of local optimization solvers. We use COBYLA as the local optimization solver within APOSMM. We give APOSMM a limit of 30,000 iterations. The limit is chosen based on an empirical observation that with this parameter choice APOSMM will restart COBYLA for at least 10 times, usually much more. Indeed, using multistart method, the results improve compared with using only COBYLA. All results are presented in Fig. 3 (a). We observe that with this small graph, even if we increase p up to 30, QAOA at most finds an estimate of the ground state up to approximation ratio 0.817. We also run QAOA experiments on slightly larger graphs, up to 10 vertices, and with p up to 10. The results of the experiments are shown in Fig. 3 (b). To compare, we run our L-VQE on each graph 10 times given different random seed. Each run is given a limit of 3,000 iterations, and we report the best result found by L-VQE in Fig. 3 (b). For each graph, L-VQE finds an estimate of the ground state with an

TABLE I: Assuming full connectivity and compiling the higher-order terms in the Hamiltonian (12) into gate sets $\{R_z, \text{CNOT}\}$, the gate count of QAOA scales quadratically with n , while L-VQE scales linearly. In our experiments presented in Fig. 3 (a), QAOA circuits with p steps consists of $77p$ single qubit gates and $336p$ CNOT gates, while L-VQE with ℓ layers contains $52\ell + 14$ single qubit gates and 26ℓ CNOT gates. Thus, we expect that the L-VQE approach will be more robust to noise in real-life experiments. CNOT count of QAOA can be decreased by further circuit optimizations and more efficient native gates. On the other hand, it would be increased if the connectivity is not full.

	QAOA with p steps	L-VQE with ℓ layers
CNOT count	$8n(n-1)p$	$\ell(4n-2)$

approximation ratio ρ of at least 0.99.

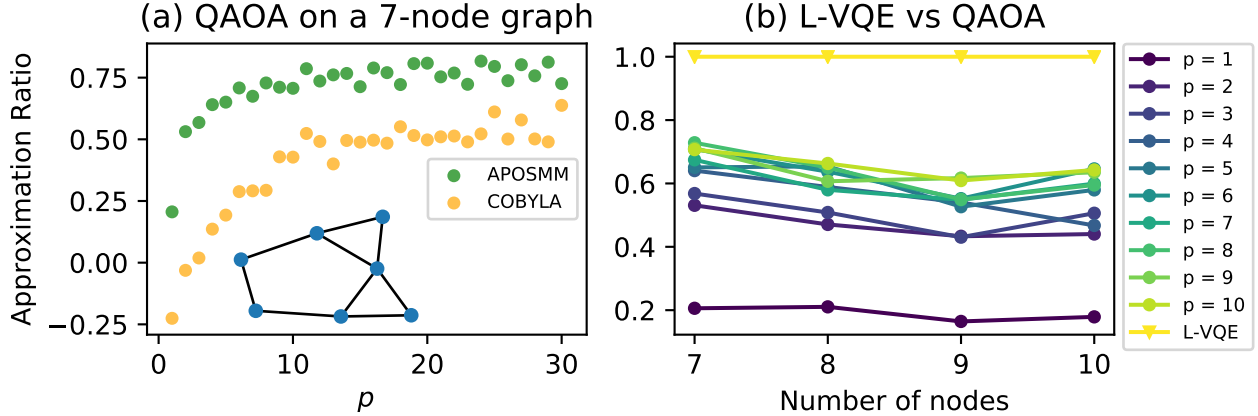


FIG. 3: (a) shows the best approximation ratio QAOA found for the 7-node graph (shown in the inset) with p ranging from 1 to 30. Even with the multistart method APOSSM to improve the optimizer COBYLA, we at most find an estimate of the ground state up to approximation ratio 0.817. (b) compares QAOA and L-VQE on graphs of size from 7 to 10, simulating 14–20 qubits. L-VQE ansatz is iteratively increased up to $\ell = 2$ layers. L-VQE finds the ground state or a state that is close (with approximation ratio at least 0.99) to the ground state for each graph.

For a graph with n vertices, our approach requires $2n$ qubits in order to detect 4 communities. Assuming full connectivity and CNOT as the entangling gate, the gate counts of QAOA and L-VQE circuits are summarized in Table I. When p is small, the Hamiltonian evolution ansatz used in QAOA is less expressive as compared with the hardware-efficient ansatz used in L-VQE. Therefore large circuit depth is needed to achieve the required overlap with the target state. At the same time, the cost function landscape of QAOA is highly nonconvex and contains many low-quality local optima, which make finding high-quality parameters difficult for larger p . In addition, the Hamiltonian (12) contains many-body terms, which makes it harder to compile into gates. The compilation is further complicated in practice by the limited connectivity of the hardware. In contrast, L-VQE follows the connectivity of the hardware, as the Hamiltonian structure does not enter the ansatz explicitly.

B. VQE and L-VQE

To further examine the performance of L-VQE, we compare the results of VQE with fixed ansatz and L-VQE on larger problems. In Section VIB 1 we compare the performance of VQE and L-VQE with sampling noise, and in Section VIB 2 we compare the performance without sampling noise. The results are summarized

TABLE II: Graph information of the `Networkx` generated instances.

Graph class	# instances	$ V $
relaxed caveman	2	20
gaussian random	2	20
random partition	4	20
windmill	1	17
gnp random	4	20
power law cluster	3	20

in Section [VIB 3](#).

We generated 16 graph instances with `NetworkX`. Graph information is summarized in Table [II](#). The goal is to find a clustering of up to 4 communities that maximizes the modularity; thus we are simulating 34 qubits for `windmill` and 40 qubits for all other graphs.

For VQE, we define a fixed form of the ansatz upfront and then iteratively optimize and update over all parameters. We compare 3 sets of ansätze, which are shown in Fig. [2](#) as Layer 0 only ($\ell = 0$), Layer 0 to 1 only ($\ell = 1$), and Layer 0 to 2 ($\ell = 2$), respectively. For L-VQE with $\ell = 0$, the ansatz will not grow; thus the algorithm is the same as VQE with one R_y gate acting on each qubit. For L-VQE with $\ell = 1$ and $\ell = 2$, we set the parameter $k_0 = 200$ in Algorithm [1](#). In other words, we first run L-VQE with Layer 0 ansatz for 200 iterations and then reuse the parameters and embed the parameters to the ansatz with 1 layer and 2 layers, respectively. Again, we run our simulations of the quantum circuits in MATLAB, with the Hamiltonian in the form of a matrix product operator [\[53\]](#). For optimization, we use the sequential minimal optimizer [\[55\]](#) and COBYLA [\[57\]](#). For each graph and each approach, we initialize the ansatz with 10 different random seeds.

1. VQE and L-VQE with sampling noise

We report the results of VQE and L-VQE with sampling noise in Table [III–VI](#). To evaluate the cost function $\langle \psi(\boldsymbol{\theta}) | \mathcal{H} | \psi(\boldsymbol{\theta}) \rangle$, we execute the circuit and generate 2,000 samples and use the mean of the samples as an estimator. Having a finite number of samples is a realistic setup, since when the scale of the system gets larger, the exact computation of the cost function becomes intractable.

In Table [III](#), we report the best approximation ratio (ρ_{best}) achieved from the 10 runs using SMO for each graph with sampling noise. In Table [IV](#), we report the average and standard deviation ($\rho_{\text{average}} \pm \sigma$) of the approximation ratio from the 10 runs for each graph. We additionally report the results that use COBYLA as the optimizer in Tables [V](#), [VI](#).

2. VQE and L-VQE without sampling noise

We report the results of VQE and L-VQE without sampling noise in Tables [VII–VIII](#). In each iteration we evaluate the cost function exactly. In Table [VII](#) we report the best approximation ratio (ρ_{best}) achieved from the 10 runs using SMO for each graph without sampling noise. In Table [VIII](#), we report the average and standard deviation ($\rho_{\text{average}} \pm \sigma$) of the approximation ratio from the 10 runs for each graph.

3. Summary of VQE and L-VQE

Across all instances we set the threshold of approximation ratio to 0.99, 0.95, and 0.90, respectively, and in Table [IX](#) we report the percentage of the local optimizer runs that find the quantum state with a higher approximation ratio at the end of the algorithm. The rows in blue are the experiments with sampling noise (i.e., the cost function is estimated by the mean of the samples), and the rows in white are the experiments without sampling noise (i.e., the cost function is evaluated exactly).

TABLE III: Best approximation ratio with sampling noise using SMO. As the number of layers in the ansatz increases, results of VQE deteriorates. L-VQE does not suffer from that problem, and we achieve better results as the number of layers grows.

graph	VQE ρ_{best}		L-VQE ρ_{best}		
	1 Layer	2 Layer	0 Layer	1 Layer	2 Layer
caveman	0.99	0.93	1.0	1.0	1.0
caveman2	0.98	0.93	0.99	0.99	0.99
gaussian	0.98	0.9	1.0	1.0	1.0
gaussian2	0.99	0.93	0.99	1.0	1.0
gnp1	0.99	0.93	1.0	1.0	1.0
gnp2	0.98	0.92	0.95	1.0	1.0
gnp3	0.99	0.91	0.99	1.0	1.0
gnp4	0.99	0.88	0.97	0.99	1.0
power	0.96	0.9	1.0	1.0	1.0
power2	0.99	0.93	0.99	1.0	1.0
power3	0.98	0.91	0.9	0.96	1.0
random1	0.98	0.93	1.0	1.0	1.0
random2	0.99	0.89	0.95	1.0	1.0
random3	0.99	0.96	1.0	1.0	1.0
random4	0.92	0.93	0.96	1.0	0.98
windmill	0.99	0.96	1.0	1.0	1.0

TABLE IV: Average approximation ratio with sampling noise using SMO. As the number of layers in the ansatz increases, results of VQE deteriorate; but for L-VQE, we achieve better results.

graph	VQE $\rho_{\text{average}} \pm \sigma$		L-VQE $\rho_{\text{average}} \pm \sigma$		
	1 Layer	2 Layer	0 Layer	1 Layer	2 Layer
caveman	0.91 ± 0.08	0.83 ± 0.08	0.83 ± 0.15	0.92 ± 0.1	0.91 ± 0.1
caveman2	0.95 ± 0.03	0.86 ± 0.06	0.92 ± 0.07	0.99 ± 0.0	0.99 ± 0.0
gaussian	0.83 ± 0.08	0.77 ± 0.09	0.86 ± 0.08	0.94 ± 0.09	0.91 ± 0.09
gaussian2	0.92 ± 0.06	0.87 ± 0.03	0.9 ± 0.07	0.95 ± 0.06	0.95 ± 0.05
gnp1	0.87 ± 0.07	0.82 ± 0.08	0.87 ± 0.07	0.93 ± 0.05	0.94 ± 0.06
gnp2	0.89 ± 0.07	0.8 ± 0.09	0.87 ± 0.07	0.92 ± 0.06	0.94 ± 0.04
gnp3	0.89 ± 0.06	0.81 ± 0.06	0.86 ± 0.07	0.94 ± 0.06	0.95 ± 0.04
gnp4	0.92 ± 0.05	0.82 ± 0.04	0.92 ± 0.05	0.95 ± 0.04	0.94 ± 0.06
power	0.9 ± 0.04	0.82 ± 0.05	0.87 ± 0.07	0.9 ± 0.07	0.89 ± 0.08
power2	0.93 ± 0.08	0.85 ± 0.06	0.9 ± 0.06	0.92 ± 0.05	0.93 ± 0.05
power3	0.85 ± 0.07	0.79 ± 0.07	0.84 ± 0.06	0.89 ± 0.04	0.9 ± 0.05
random1	0.91 ± 0.1	0.84 ± 0.05	0.86 ± 0.13	0.98 ± 0.02	0.98 ± 0.02
random2	0.93 ± 0.07	0.81 ± 0.06	0.85 ± 0.1	0.93 ± 0.07	0.93 ± 0.06
random3	0.95 ± 0.05	0.84 ± 0.1	0.9 ± 0.11	0.95 ± 0.04	0.97 ± 0.03
random4	0.85 ± 0.05	0.83 ± 0.07	0.82 ± 0.08	0.9 ± 0.08	0.9 ± 0.07
windmill	0.93 ± 0.06	0.9 ± 0.05	0.84 ± 0.12	0.92 ± 0.06	0.94 ± 0.06

Intuitively, when we increase the size of the ansatz, the ansatz becomes more expressive, and we should have a better chance of finding the ground state. However, we can see that for VQE, with sampling noise, as the number of layers in the ansatz increase, the results deteriorate. But for L-VQE, as we increase the size of the ansatz, the results improve. Moreover, it is not practical to evaluate the energy exactly in applications when the size of the system gets larger. In L-VQE, by reusing parameters and by using the optimization process, we can achieve a higher probability of finding the ground state or a state that is sufficiently close to the ground state. By comparing the results of our L-VQE with or without sampling noise, we can see no significant difference, which suggests that our approach is relatively robust to sampling noise.

We further investigate the effect of reusing parameters and adding layers of the ansatz in L-VQE; the results are summarized in Table III - VIII. We observe that for the runs of experiments that start from the

TABLE V: Best approximation ratio with sampling noise using COBYLA. As the number of layers in the ansatz increases, results of VQE deteriorate; but for L-VQE, we achieve better results. Thus L-VQE is more robust under sampling noise compared with VQE.

graph	VQE ρ_{best}		L-VQE ρ_{best}		
	1 Layer	2 Layer	0 Layer	1 Layer	2 Layer
caveman	0.96	0.89	0.97	1.0	1.0
caveman2	0.95	0.92	0.97	0.99	0.99
gaussian	0.96	0.81	0.92	1.0	1.0
gaussian2	0.91	0.84	0.91	1.0	1.0
gnp1	0.94	0.85	0.91	1.0	1.0
gnp2	0.86	0.84	0.87	0.97	0.97
gnp3	0.83	0.84	0.97	1.0	1.0
gnp4	0.89	0.86	0.96	1.0	0.98
power	0.89	0.89	0.92	0.99	0.99
power2	0.91	0.77	0.9	1.0	1.0
power3	0.92	0.83	0.91	1.0	1.0
random1	0.93	0.88	0.96	1.0	1.0
random2	0.92	0.91	0.93	1.0	1.0
random3	0.97	0.91	0.98	1.0	1.0
random4	0.91	0.88	0.91	1.0	1.0
windmill	0.97	0.95	0.99	1.0	1.0

TABLE VI: Average approximation ratio with sampling noise using COBYLA. As the number of layers in the ansatz increases, results of VQE deteriorate, but for L-VQE, we achieve better results. Thus L-VQE is more robust under sampling noise compared with VQE.

graph	conventional VQE $\rho_{\text{average}} \pm \sigma$		L-VQE $\rho_{\text{average}} \pm \sigma$		
	1 Layer	2 Layer	0 Layer	1 Layer	2 Layer
caveman	0.86 ± 0.07	0.81 ± 0.06	0.8 ± 0.1	0.9 ± 0.07	0.88 ± 0.06
caveman2	0.84 ± 0.09	0.77 ± 0.12	0.82 ± 0.13	0.98 ± 0.02	0.99 ± 0.0
gaussian	0.76 ± 0.15	0.63 ± 0.1	0.75 ± 0.08	0.89 ± 0.08	0.87 ± 0.07
gaussian2	0.78 ± 0.1	0.69 ± 0.09	0.8 ± 0.08	0.96 ± 0.05	0.97 ± 0.04
gnp1	0.8 ± 0.08	0.72 ± 0.09	0.79 ± 0.09	0.9 ± 0.06	0.91 ± 0.07
gnp2	0.75 ± 0.07	0.72 ± 0.1	0.78 ± 0.07	0.91 ± 0.06	0.92 ± 0.05
gnp3	0.69 ± 0.1	0.71 ± 0.1	0.79 ± 0.11	0.93 ± 0.06	0.94 ± 0.07
gnp4	0.81 ± 0.08	0.71 ± 0.11	0.85 ± 0.06	0.95 ± 0.03	0.95 ± 0.03
power	0.79 ± 0.07	0.67 ± 0.14	0.76 ± 0.1	0.92 ± 0.05	0.92 ± 0.03
power2	0.78 ± 0.1	0.67 ± 0.08	0.78 ± 0.09	0.95 ± 0.03	0.93 ± 0.07
power3	0.77 ± 0.1	0.67 ± 0.07	0.79 ± 0.09	0.9 ± 0.08	0.86 ± 0.08
random1	0.82 ± 0.09	0.74 ± 0.12	0.86 ± 0.09	0.98 ± 0.03	0.97 ± 0.03
random2	0.78 ± 0.12	0.69 ± 0.15	0.82 ± 0.08	0.93 ± 0.05	0.95 ± 0.04
random3	0.84 ± 0.1	0.79 ± 0.1	0.9 ± 0.06	0.94 ± 0.04	0.94 ± 0.05
random4	0.8 ± 0.09	0.71 ± 0.08	0.77 ± 0.09	0.93 ± 0.06	0.94 ± 0.05
windmill	0.9 ± 0.06	0.82 ± 0.09	0.87 ± 0.09	0.92 ± 0.06	0.92 ± 0.06

same initial Layer 0 ansatz, by reusing the parameters obtained from that ansatz, in most cases the results improve. Across all runs of the experiments, with sampling noise, for 1 layer, 147 out of the 160 (91.88%) runs find a state with a better or equal approximation ratio compared with the ansatz with 0 layer only. For 2 layers, 151 out of the 160 (94.38%) runs find a state with a better or equal approximation ratio compared with the ansatz with 0 layers. Similarly, without sampling noise, across all runs of the experiments, for 1 layer, 150 out of the 160 (93.75%) runs find a state with a better or equal approximation ratio compared with the ansatz with 0 layers. For 2 layers, 151 out of the 160 (94.38%) runs find a quantum state with a better or equal approximation ratio compared with the ansatz with 0 layer.

TABLE VII: Best approximation ratio without sampling noise using SMO. L-VQE is clearly more robust under sampling noise compared with VQE.

graph	VQE ρ_{best}		L-VQE ρ_{best}		
	1 Layer	2 Layer	0 Layer	1 Layer	2 Layer
caveman	1.0	1.0	0.95	1.0	1.0
caveman2	0.99	0.99	0.99	0.99	0.99
gaussian	1.0	1.0	1.0	1.0	1.0
gaussian2	1.0	1.0	1.0	1.0	1.0
gnp1	1.0	0.94	1.0	1.0	1.0
gnp2	0.97	1.0	0.92	0.97	1.0
gnp3	1.0	1.0	1.0	1.0	0.99
gnp4	1.0	1.0	0.99	1.0	0.98
power	0.94	0.93	0.98	0.99	1.0
power2	1.0	1.0	0.99	1.0	1.0
power3	0.96	0.96	0.9	1.0	1.0
random1	1.0	1.0	0.97	1.0	1.0
random2	1.0	1.0	0.98	1.0	1.0
random3	1.0	1.0	1.0	1.0	1.0
random4	0.98	0.97	1.0	1.0	1.0
windmill	1.0	1.0	1.0	1.0	1.0

TABLE VIII: Average approximation ratio without sampling noise using SMO. L-VQE is clearly more robust under sampling noise compared with VQE.

graph	VQE $\rho_{\text{average}} \pm \sigma$		L-VQE $\rho_{\text{average}} \pm \sigma$		
	1 Layer	2 Layer	0 Layer	1 Layer	2 Layer
caveman	0.89 ± 0.12	0.92 ± 0.06	0.76 ± 0.11	0.9 ± 0.09	0.92 ± 0.09
caveman2	0.96 ± 0.04	0.96 ± 0.07	0.92 ± 0.06	0.99 ± 0.0	0.99 ± 0.0
gaussian	0.94 ± 0.07	0.92 ± 0.08	0.81 ± 0.08	0.94 ± 0.09	0.85 ± 0.08
gaussian2	0.97 ± 0.05	0.99 ± 0.02	0.86 ± 0.1	0.99 ± 0.04	0.97 ± 0.04
gnp1	0.94 ± 0.04	0.89 ± 0.04	0.88 ± 0.08	0.92 ± 0.05	0.9 ± 0.05
gnp2	0.9 ± 0.05	0.94 ± 0.04	0.89 ± 0.03	0.92 ± 0.05	0.92 ± 0.05
gnp3	0.92 ± 0.08	0.88 ± 0.06	0.89 ± 0.06	0.9 ± 0.07	0.92 ± 0.06
gnp4	0.94 ± 0.03	0.95 ± 0.05	0.88 ± 0.07	0.96 ± 0.03	0.92 ± 0.06
power	0.91 ± 0.04	0.9 ± 0.03	0.87 ± 0.07	0.92 ± 0.08	0.89 ± 0.08
power2	0.95 ± 0.04	0.93 ± 0.06	0.91 ± 0.08	0.94 ± 0.05	0.92 ± 0.08
power3	0.84 ± 0.08	0.89 ± 0.06	0.82 ± 0.08	0.91 ± 0.05	0.92 ± 0.05
random1	0.87 ± 0.14	0.97 ± 0.02	0.92 ± 0.06	0.97 ± 0.02	0.98 ± 0.02
random2	0.96 ± 0.04	0.95 ± 0.06	0.9 ± 0.06	0.96 ± 0.03	0.97 ± 0.02
random3	0.96 ± 0.08	0.95 ± 0.07	0.9 ± 0.11	0.97 ± 0.04	0.96 ± 0.04
random4	0.89 ± 0.06	0.91 ± 0.05	0.8 ± 0.12	0.94 ± 0.08	0.94 ± 0.06
windmill	0.96 ± 0.06	0.94 ± 0.06	0.82 ± 0.12	0.96 ± 0.06	0.96 ± 0.06

C. Further Evidence of the Potential of L-VQE

To provide further evidence of the potential of L-VQE, we present a scaling analysis of L-VQE in Section VIC1 and discuss the simulation results of L-VQE on a trapped ion noisy quantum simulator in Section VIC2.

TABLE IX: Percentage of runs of local optimizers that reach a given approximation ratio: blue rows show results from experiments with sampling noise; white rows are from experiments without sampling noise. The optimizer is SMO. With sampling noise, as the number of layers in the ansatz increases, results of VQE deteriorate. But for L-VQE, we achieve better results. Thus L-VQE is more robust under sampling noise compared with VQE.

Approximation ratio > 0.99	0 Layer	1 Layer	2 Layer
VQE	11.875%	0.625%	0.0%
L-VQE	11.875%	29.375%	30.625%
VQE	7.5%	26.875%	24.375%
L-VQE	7.5%	31.25%	27.5%
Approximation ratio > 0.95	0 Layer	1 Layer	2 Layer
VQE	21.25%	33.75%	1.25%
L-VQE	21.25%	49.375%	48.125%
VQE	18.75%	45.0%	48.125%
L-VQE	18.75%	57.5%	58.125%
Approximation ratio > 0.90	0 Layer	1 Layer	2 Layer
VQE	40.0%	55%	19.375%
L-VQE	40.0%	66.875%	67.5%
VQE	42.5%	72.5%	66.25%
L-VQE	42.5%	71.25%	71.25%

1. Scaling analysis

In this set of experiments, we generate random graphs with vertices ranging from 8 to 20. This means that in our application of finding a clustering up to 4 communities that maximize the modularity, we need to simulate qubits ranging from 16 to 40. For each graph and each approach, we run the experiments 10 times and record the average number of iterations needed for convergence of each graph. The results are shown in Fig. 4. We can see that the number of iterations scales up polynomially as the number of vertices increases. Here, since within each iteration the number of R_y gates in the ansatz scales linearly with respect to the number of qubits needed (ansatz shown in Fig. 2), the number of parameters that need to be optimized therefore scales up linearly. In addition, the number of samples produced for evaluating the cost function is fixed as constant. Thus, the resources required for the entire algorithm scale polynomially. We point out, however, that our algorithm is heuristic by design and there is no guarantee of obtaining a solution with specified quality.

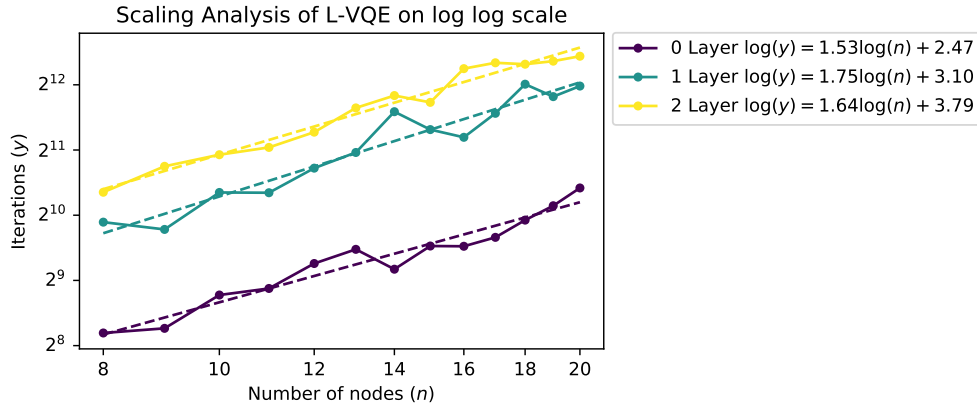


FIG. 4: Average number of iterations until convergence scales up polynomially with respect to the size of the graph.

2. Noisy simulations

The experiments described in the preceding sections are simulated in a setting that has no gate noise, but we do simulate sampling noise in some cases. For demonstration purposes, in the next set of experiments we also investigate the performance of L-VQE using a trapped ion noisy quantum simulator. We use realistic error rates in our simulations. Details of the noise model are given in Appendix C of [63] and in [64]. We run the experiments on a **caveman** graph with 20 nodes. For L-VQE with Layer 1 and Layer 2, we run the experiments 10 times each. Fig. 5 gives a violin plot of the results. We observe that as the size of the ansatz increases, the probability of finding the ground state or a state that is sufficiently close increases. This suggests that L-VQE is also relatively robust to hardware noise and can be adapted to different quantum architectures.

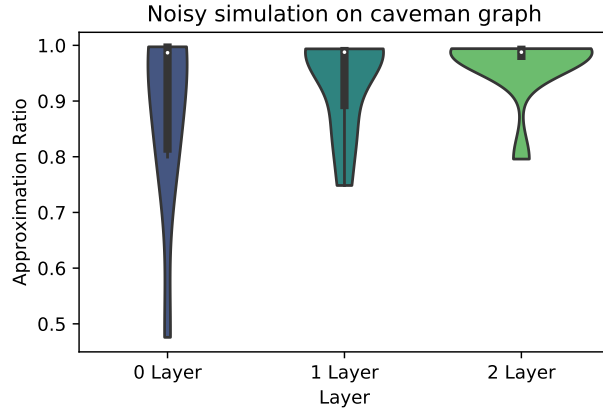


FIG. 5: Violin plot of L-VQE performance on a trapped ion noisy quantum simulator. The plot shows the probability density of the results, with the kernel density estimator truncated to $(\min(\rho), \max(\rho))$ (since the approximation ratio cannot exceed 1). As the size of the ansatz increases, the probability of finding the ground state or a state that is sufficiently close increases.

D. Entanglement vs no entanglement

Our next experiment is aimed at understanding the role of entanglement in VQE. We use the same methodology as proposed in [8]. That is, the experiment is based on replacing the entanglement gates CNOT with a T gate acting on both qubits. Compared with previous work, with our simulator we can investigate the algorithm’s performance on larger problems. We run the experiments on 4 graphs: (**caveman**, **gnp**, **random**, and **gaussian**). For each graph, we repeat the experiments 10 times with a different random seed. For the set of experiments with entanglement, we use the ansatz described in Fig. 2 with Layer 0 and Layer 1. For the set of experiments without entanglement, we replace all CNOT gates with a T gate acting on both qubits. The results are summarized in Table X, where we report the percentage of runs that reach the approximation threshold 0.99, 0.95, and 0.90, respectively. As we can see from the results, under both cases, with sampling noise and without, using the ansatz with entanglement performs better than using the ansatz without entanglement.

VII. CONCLUSIONS AND DISCUSSION

Combinatorial optimization on near-term quantum devices is a leading candidate to demonstrate quantum advantage, and hybrid quantum-classical algorithms have been developed to solve this problem. In this work,

TABLE X: Percentage of experiments given the approximation ratio threshold

Approximation ratio > 0.99	Entanglement	No entanglement
With sampling noise	15%	0%
Without sampling noise	37.5%	32.5%
Approximation ratio > 0.95	Entanglement	No entanglement
With sampling noise	45%	37.5%
Without sampling noise	57.5%	47.5%
Approximation ratio > 0.90	Entanglement	No entanglement
With sampling noise	65%	60%
Without sampling noise	70%	57.5%

we propose an iterative L-VQE approach inspired by VQE. We specifically studied the application of k -communities detection. In existing works, for a graph with n vertices, solving the k -communities modularity maximization problem requires kn qubits that encode the problem as an Ising model Hamiltonian. We propose a novel qubit-frugal formulation that requires only $n \lceil \log k \rceil$ qubits.

We compared the performance of L-VQE with QAOA, which is widely considered to be strong candidate for quantum advantage in applications with NISQ computers. However, the many-body terms in the Hamiltonian make it harder to implement in the QAOA setting. Moreover, the numerical results show that the optimization indeed gets harder, thus suggesting that L-VQE provides a practical alternative to QAOA for combinatorial optimization on noisy near-term quantum computers.

Unlike VQE, which has an ansatz fixed upfront, L-VQE starts from a simple and shallow hardware efficient ansatz with a small number of parameterized gates and then adds layers to the ansatz systematically. This strategy allows us to make the ansatz more expressive and reduces the optimization overhead. Our numerical results suggest that adding layers of the ansatz indeed increases the probability of finding the ground state or finding the state that is sufficiently close to the ground state. With the presence of sampling noise, however, VQE is more likely to fail. We empirically observe L-VQE to be more robust under sampling noise, making it a promising approach for NISQ devices. We use matrix product state representation to perform large-scale simulations of the quantum circuits in MATLAB. Doing so allowed us to explore problems of larger size (simulations up to 40 qubits and 352 parameters). We also studied the performance of L-VQE using a simulator of noisy trapped-ion quantum computer. The results suggest that our approach is relatively robust to hardware noise and can be adapted and generalized to different quantum architectures. Finally, we present numerical results of the role of entanglement in VQE. The results clearly show that the ansatz with entanglement performs better than the ansatz without entanglement.

Our results are the first indication that the introduction of additional entangling parameters in VQE for classical problems, as proposed in [65, Section V-B], break down the barriers in the optimization landscape, making it more convex and therefore more amenable to simple local outer-loop optimizers to find a minimum. This is in sharp contrast with the previous results of Nannicini [8], who did not observe any beneficial effects of entanglement. The difference in findings between our results and those presented in [8] suggests the importance of the parameterization choice and the overall VQE procedure design to the success of such methods. We hope that this work will lead to even better algorithms to design ansätze for NISQ devices.

ACKNOWLEDGMENTS

We thank Jeffrey Larson for help with tuning APOSMM for QAOA parameter optimization. Clemson University is acknowledged for generous allotment of compute time on the Palmetto cluster. X.L., A.A., R.S., I.S. and Y.A. were supported in part with funding from the Defense Advanced Research Projects Agency (DARPA). R.S. and Y.A. were supported by Laboratory Directed Research and Development (LDRD) funding from Argonne National Laboratory, provided by the Director, Office of Science, of the U.S. Department of Energy under Contract No. DE-AC02-06CH11357. R.S. was supported by the U.S. Department of Energy, Office of Science, Office of Advanced Scientific Computing Research, Accelerated Research for Quantum Computing program. L.C. was supported by the Laboratory Directed Research and Development (LDRD)

program of Los Alamos National Laboratory (LANL) under project number 20200056DR. LANL is operated by Triad National Security, LLC, for the National Nuclear Security Administration of U.S. Department of Energy (contract no. 89233218CNA000001). L.C. was also supported by the U.S. DOE, Office of Science, Office of Advanced Scientific Computing Research, under the Accelerated Research in Quantum Computing (ARQC) program.

-
- [1] Y. Alexeev, D. Bacon, K. R. Brown, R. Calderbank, L. D. Carr, F. T. Chong, B. DeMarco, D. Englund, E. Farhi, B. Fefferman, *et al.*, Quantum computer systems for scientific discovery, [arXiv preprint arXiv:1912.07577 \(2019\)](#).
 - [2] R. Shaydulin, H. Ushijima-Mwesigwa, C. F. A. Negre, I. Safro, S. M. Mniszewski, and Y. Alexeev, A hybrid approach for solving optimization problems on small quantum computers, *Computer* **52**, 18 (2019).
 - [3] J. Preskill, Quantum computing in the NISQ era and beyond, *Quantum* **2**, 79 (2018).
 - [4] E. Farhi, J. Goldstone, and S. Gutmann, A quantum approximate optimization algorithm, [arXiv preprint arXiv:1411.4028 \(2014\)](#).
 - [5] S. Hadfield, Z. Wang, B. O’Gorman, E. Rieffel, D. Venturelli, and R. Biswas, From the quantum approximate optimization algorithm to a quantum alternating operator ansatz, *Algorithms* **12**, 34 (2019).
 - [6] E. Farhi, J. Goldstone, S. Gutmann, and H. Neven, Quantum algorithms for fixed qubit architectures, [arXiv preprint arXiv:1703.06199 \(2017\)](#).
 - [7] L. Zhu, H. L. Tang, G. S. Barron, N. J. Mayhall, E. Barnes, and S. E. Economou, An adaptive quantum approximate optimization algorithm for solving combinatorial problems on a quantum computer, [arXiv preprint arXiv:2005.10258 \(2020\)](#).
 - [8] G. Nannicini, Performance of hybrid quantum-classical variational heuristics for combinatorial optimization, *Physical Review E* **99**, 013304 (2019).
 - [9] M. Cerezo, A. Arrasmith, R. Babbush, S. C. Benjamin, S. Endo, K. Fujii, J. R. McClean, K. Mitarai, X. Yuan, L. Cincio, *et al.*, Variational quantum algorithms, [arXiv preprint arXiv:2012.09265 \(2020\)](#).
 - [10] Z. Holmes, K. Sharma, M. Cerezo, and P. J. Coles, Connecting ansatz expressibility to gradient magnitudes and barren plateaus, [arXiv preprint arXiv:2101.02138 \(2021\)](#).
 - [11] J. R. McClean, S. Boixo, V. N. Smelyanskiy, R. Babbush, and H. Neven, Barren plateaus in quantum neural network training landscapes, *Nature communications* **9**, 1 (2018).
 - [12] A. Kandala, A. Mezzacapo, K. Temme, M. Takita, M. Brink, J. M. Chow, and J. M. Gambetta, Hardware-efficient variational quantum eigensolver for small molecules and quantum magnets, *Nature* **549**, 242 (2017).
 - [13] R. Shaydulin, S. Hadfield, T. Hogg, and I. Safro, Classical symmetries and QAOA, [arXiv preprint arXiv:2012.04713 \(2020\)](#).
 - [14] S. Bravyi, A. Kliesch, R. Koenig, and E. Tang, Obstacles to state preparation and variational optimization from symmetry protection, [arXiv preprint arXiv:1910.08980 \(2019\)](#).
 - [15] M. Cerezo, A. Sone, T. Volkoff, L. Cincio, and P. J. Coles, Cost-function-dependent barren plateaus in shallow quantum neural networks, [arXiv preprint arXiv:2001.00550 \(2020\)](#).
 - [16] K. Sharma, M. Cerezo, L. Cincio, and P. J. Coles, Trainability of dissipative perceptron-based quantum neural networks, [arXiv preprint, arXiv:2005.12458 \(2020\)](#).
 - [17] A. Pesah, M. Cerezo, S. Wang, T. Volkoff, A. T. Sornborger, and P. J. Coles, Absence of barren plateaus in quantum convolutional neural networks, [arXiv preprint, arXiv:2011.02966 \(2020\)](#).
 - [18] M. Cerezo and P. J. Coles, Impact of barren plateaus on the Hessian and higher order derivatives, [arXiv preprint, arXiv:2008.07454 \(2020\)](#).
 - [19] S. Wang, E. Fontana, M. Cerezo, K. Sharma, A. Sone, L. Cincio, and P. J. Coles, Noise-induced barren plateaus in variational quantum algorithms, [arXiv preprint, arXiv:2007.14384 \(2020\)](#).
 - [20] Z. Holmes, A. Arrasmith, B. Yan, P. J. Coles, A. Albrecht, and A. T. Sornborger, Barren plateaus preclude learning scramblers, [arXiv preprints, arXiv:2009.14808 \(2020\)](#).
 - [21] T. J. Volkoff, Efficient trainability of linear optical modules in quantum optical neural networks, [arXiv preprint, arXiv:2008.09173 \(2020\)](#).
 - [22] E. Campos, A. Nasrallah, and J. Biamonte, Abrupt transitions in variational quantum circuit training, [arXiv preprint, arXiv:2010.09720 \(2020\)](#).
 - [23] C. Ortiz Marrero, M. Kieferová, and N. Wiebe, Entanglement induced barren plateaus, [arXiv preprint, arXiv:2010.15968 \(2020\)](#).
 - [24] A. Abbas, D. Sutter, C. Zoufal, A. Lucchi, A. Figalli, and S. Woerner, The power of quantum neural networks, [arXiv preprint, arXiv:2011.00027 \(2020\)](#).

- [25] S. Khairy, R. Shaydulin, L. Cincio, Y. Alexeev, and P. Balaprakash, Learning to optimize variational quantum circuits to solve combinatorial problems, *Proceedings of the Thirty-Forth AAAI Conference on Artificial Intelligence (AAAI-20)* (2019).
- [26] M. Wilson, S. Stromswold, F. Wudarski, S. Hadfield, N. M. Tubman, and E. Rieffel, Optimizing quantum heuristics with meta-learning, *arXiv preprint arXiv:1908.03185* (2019).
- [27] G. Verdon, M. Broughton, J. R. McClean, K. J. Sung, R. Babbush, Z. Jiang, H. Neven, and M. Mohseni, Learning to learn with quantum neural networks via classical neural networks, *arXiv preprint arXiv:1907.05415* (2019).
- [28] L. Zhou, S.-T. Wang, S. Choi, H. Pichler, and M. D. Lukin, Quantum approximate optimization algorithm: Performance, mechanism, and implementation on near-term devices, *Physical Review X* **10**, 021067 (2020).
- [29] G. E. Crooks, Performance of the quantum approximate optimization algorithm on the maximum cut problem, *arXiv preprint arXiv:1811.08419* (2018).
- [30] G. B. Mbeng, R. Fazio, and G. Santoro, Quantum annealing: A journey through digitalization, control, and hybrid quantum variational schemes, *arXiv preprint arXiv:1906.08948* (2019).
- [31] H. R. Grimsley, S. E. Economou, E. Barnes, and N. J. Mayhall, An adaptive variational algorithm for exact molecular simulations on a quantum computer, *Nature communications* **10**, 1 (2019).
- [32] A. Skolik, J. R. McClean, M. Mohseni, P. van der Smagt, and M. Leib, Layerwise learning for quantum neural networks, *arXiv preprint arXiv:2006.14904* (2020).
- [33] A. Peruzzo, J. McClean, P. Shadbolt, M.-H. Yung, X.-Q. Zhou, P. J. Love, A. Aspuru-Guzik, and J. L. O’Brien, A variational eigenvalue solver on a photonic quantum processor, *Nature communications* **5**, 4213 (2014).
- [34] M. Paredes Quinones and C. Junqueira, Modeling Linear Inequality Constraints in Quadratic Binary Optimization for Variational Quantum Eigensolver, *arXiv preprint arXiv:2007.13245* (2020).
- [35] P. K. Barkoutsos, G. Nannicini, A. Robert, I. Tavernelli, and S. Woerner, Improving variational quantum optimization using CVaR, *Quantum* **4**, 256 (2020).
- [36] M. Streif and M. Leib, Training the quantum approximate optimization algorithm without access to a quantum processing unit, *Quantum Science and Technology* **5**, 034008 (2020).
- [37] R. Shaydulin and S. M. Wild, Exploiting symmetry reduces the cost of training qaoa, *arXiv preprint arXiv:2101.10296* (2021).
- [38] F. G. Brandao, M. Broughton, E. Farhi, S. Gutmann, and H. Neven, For fixed control parameters the quantum approximate optimization algorithm’s objective function value concentrates for typical instances, *arXiv preprint arXiv:1812.04170* (2018).
- [39] R. Shaydulin, I. Safro, and J. Larson, Multistart methods for quantum approximate optimization, in *2019 IEEE High Performance Extreme Computing Conference (HPEC)* (IEEE, 2019) pp. 1–8.
- [40] M. E. Newman, Modularity and community structure in networks, *Proceedings of the national academy of sciences* **103**, 8577 (2006).
- [41] A. M. Niklasson, S. M. Mniszewski, C. F. Negre, M. J. Cawkwell, P. J. Swart, J. Mohd-Yusof, T. C. Germann, M. E. Wall, N. Bock, E. H. Rubensson, *et al.*, Graph-based linear scaling electronic structure theory, *The Journal of Chemical Physics* **144**, 234101 (2016).
- [42] H. Jeong, B. Tombor, R. Albert, Z. N. Oltvai, and A.-L. Barabási, The large-scale organization of metabolic networks, *Nature* **407**, 651 (2000).
- [43] J. Ugander, B. Karrer, L. Backstrom, and C. Marlow, The anatomy of the Facebook social graph, *arXiv preprint arXiv:1111.4503* (2011).
- [44] U. Brandes, D. Delling, M. Gaertler, R. Görke, M. Hofer, Z. Nikoloski, and D. Wagner, Maximizing modularity is hard, *arXiv preprint arXiv:physics/0608255* (2006).
- [45] S. Wang, E. Fontana, M. Cerezo, K. Sharma, A. Sone, L. Cincio, and P. J. Coles, Noise-induced barren plateaus in variational quantum algorithms, *arXiv preprint arXiv:2007.14384* (2020).
- [46] C. Xue, Z.-Y. Chen, Y.-C. Wu, and G.-P. Guo, Effects of quantum noise on quantum approximate optimization algorithm, *arXiv preprint arXiv:1909.02196* (2019).
- [47] M. C. Nascimento and A. C. De Carvalho, Spectral methods for graph clustering—a survey, *European Journal of Operational Research* **211**, 221 (2011).
- [48] C. F. Negre, H. Ushijima-Mwesigwa, and S. M. Mniszewski, Detecting multiple communities using quantum annealing on the D-Wave system, *Plos one* **15**, e0227538 (2020).
- [49] R. Shaydulin, H. Ushijima-Mwesigwa, I. Safro, S. Mniszewski, and Y. Alexeev, Network community detection on small quantum computers, *Advanced Quantum Technologies* **2**, 1900029 (2019).
- [50] H. Ushijima-Mwesigwa, C. F. Negre, and S. M. Mniszewski, Graph partitioning using quantum annealing on the D-Wave system, in *Proceedings of the Second International Workshop on Post Moores Era Supercomputing* (2017) pp. 22–29.
- [51] H. Ushijima-Mwesigwa, R. Shaydulin, C. F. Negre, S. M. Mniszewski, Y. Alexeev, and I. Safro, Multilevel combinatorial optimization across quantum architectures, *to appear in ACM Transactions on Quantum Computing*, *arXiv preprint arXiv:1910.09985* (2019).

- [52] R. Shaydulin, H. Ushijima-Mwesigwa, I. Safro, S. Mniszewski, and Y. Alexeev, Community detection across emerging quantum architectures, *Proceedings of the 3rd International Workshop on Post Moore's Era Supercomputing* (2018).
- [53] R. Orús, A practical introduction to tensor networks: Matrix product states and projected entangled pair states, *Annals of Physics* **349**, 117 (2014).
- [54] D. Lykov, R. Schutski, A. Galda, V. Vinokur, and Y. Alexeev, Tensor network quantum simulator with step-dependent parallelization, *arXiv preprint arXiv:2012.02430* (2020).
- [55] K. M. Nakanishi, K. Fujii, and S. Todo, Sequential minimal optimization for quantum-classical hybrid algorithms, *arXiv preprint arXiv:1903.12166* (2019).
- [56] *Qiskit: An open-source framework for quantum computing* (2019).
- [57] M. J. Powell, A direct search optimization method that models the objective and constraint functions by linear interpolation, in *Advances in optimization and numerical analysis* (Springer, 1994) pp. 51–67.
- [58] M. J. D. Powell, Direct search algorithms for optimization calculations, *Acta Numerica* **7**, 287 (1998).
- [59] E. Jones, T. Oliphant, P. Peterson, *et al.*, *SciPy: Open source scientific tools for Python* (2001–), [Online].
- [60] S. Hudson, J. Larson, S. M. Wild, and D. Bindel, *libEnsemble users manual* (2019).
- [61] J. Larson and S. M. Wild, A batch, derivative-free algorithm for finding multiple local minima, *Optimization and Engineering* **17**, 205 (2016).
- [62] J. Larson and S. M. Wild, Asynchronously parallel optimization solver for finding multiple minima, *Mathematical Programming Computation* **10**, 303 (2018).
- [63] L. Cincio, K. Rudinger, M. Sarovar, and P. J. Coles, Machine learning of noise-resilient quantum circuits, *arXiv preprint arXiv:2007.01210* (2020).
- [64] C. J. Trout, M. Li, M. Gutiérrez, Y. Wu, S.-T. Wang, L. Duan, and K. R. Brown, Simulating the performance of a distance-3 surface code in a linear ion trap, *New Journal of Physics* **20**, 043038 (2018).
- [65] J. R. McClean, M. P. Harrigan, M. Mohseni, N. C. Rubin, Z. Jiang, S. Boixo, V. N. Smelyanskiy, R. Babbush, and H. Neven, Low depth mechanisms for quantum optimization, *arXiv preprint arXiv:2008.08615* (2020).

The submitted manuscript has been created by UChicago Argonne, LLC, Operator of Argonne National Laboratory (“Argonne”). Argonne, a U.S. Department of Energy Office of Science laboratory, is operated under Contract No. DE-AC02-06CH11357. The U.S. Government retains for itself, and others acting on its behalf, a paid-up nonexclusive, irrevocable worldwide license in said article to reproduce, prepare derivative works, distribute copies to the public, and perform publicly and display publicly, by or on behalf of the Government. The Department of Energy will provide public access to these results of federally sponsored research in accordance with the DOE Public Access Plan <http://energy.gov/downloads/doe-public-access-plan>.